

Examination of the Combustion Process in an SI Engine Using New Characteristic Values of the Combustion Pressure and the Monochromatic Radiation

K.Gebauer and H.Müller

*Technische Universität Braunschweig
Institut für Verbrennungskraftmaschinen und Flugtriebwerke
Langer Kamp 6, 38106 Braunschweig
Germany*

ABSTRACT

Combustion in an SI engine will be examined, using the combustion pressure (CP) and the combustion radiation (CR). The objective is to determine characteristics of these combustion signals which can be used to control the relative air/fuel ratio (λ) or the rate of exhaust gas recirculation (EGR).

From the cylinder pressure, the combustion process will be calculated, divided into the inflammation period (IP), the main conversion period (MCP) and the post burning period (PBP) [1]. This identifies the point at which 50% of the available energy has been converted, designated in degrees of crank angle ($^{\circ}$ CA) as the position of the MCP. This extensive calculation [2] will be simplified by the use of a new calculation model, and a characteristic value derived from it. This value can be calculated as accurately as α_{E50} , but much more quickly.

The CR will be examined both as a whole and broken down spectrally. The results are characteristics which give a statement corresponding to the combustion process which is calculated from the CP. This statement can be used to determine the operating limit for conditions of high λ or high rates of EGR.

Two new characteristics which are calculated from the CP and from the monochromatic CR contribute greatly to the control of λ or the rate of EGR. This allows improvement of SI engine efficiency, as well as minimization of pollutant emissions.

INTRODUCTION

Special measures are required for operation of SI engines in order to comply with the latest emission standards. Emission limits like those desired for Low-Emission Vehicles (LEV), and Ultra-Low-Emission Vehicles (ULEV) [3] are only possible with the simultaneous use of EGR and a three-way catalytic converter. Optimal functioning of the catalytic converter requires $\lambda = 1.0$. Effective joint use of a catalytic converter

and EGR requires the utilization of variables which, since they must be precise, must be taken directly from the combustion process.

The examination of the CP, as well as the thermodynamic calculation of the energy conversion computed from it, are used for the evaluation because of their high degree of accuracy. Using this model, the combustion process is divided into three periods:

- IP which is defined as the time, in $^{\circ}$ CA, needed from ignition timing (α_{IG}) until 1% of the energy has been converted,
- MCP which is defined as the time, in $^{\circ}$ CA, needed from 1% to 90% of the converted energy,
- PBP which is defined as the time, in $^{\circ}$ CA, after 90% of the energy has been converted until the combustion is finished.

The crank position of 1% of converted energy (α_{E1}), marking the end of IP, and the crank position of 50% of converted energy (α_{E50}), marking the position of MCP, are essential values used during the combustion process.

The computer for on-board management (OBM), which is used to control the engine, and is required in order to meet the newest regulations [4], is not capable of handling the thermodynamic examination of the CP. Reaction from one cycle to the next is impossible because of the extensive calculations it requires. Therefore, a calculation model has been developed which allows the ready calculation of a value whose usability and accuracy are similar to α_{E50} .

COMBUSTION PRESSURE

A reliable, inexpensive and thermoshock-resistant pressure transducer is required in order to measure the CP.

Fundamentals

At this point an important expression related to α_{IG} must be explained. It is common practice to set α_{IG} - dependant upon engine speed, load, λ and rate of EGR - to its "unrestricted" optimum position in order to achieve the highest efficiency. This implies that α_{IG} is required earlier in order to keep α_{E50} at a constant position, if for example, an increasing λ lengthens the IP due to the decreasing

* Numbers in brackets designate references listed at the end of this paper.

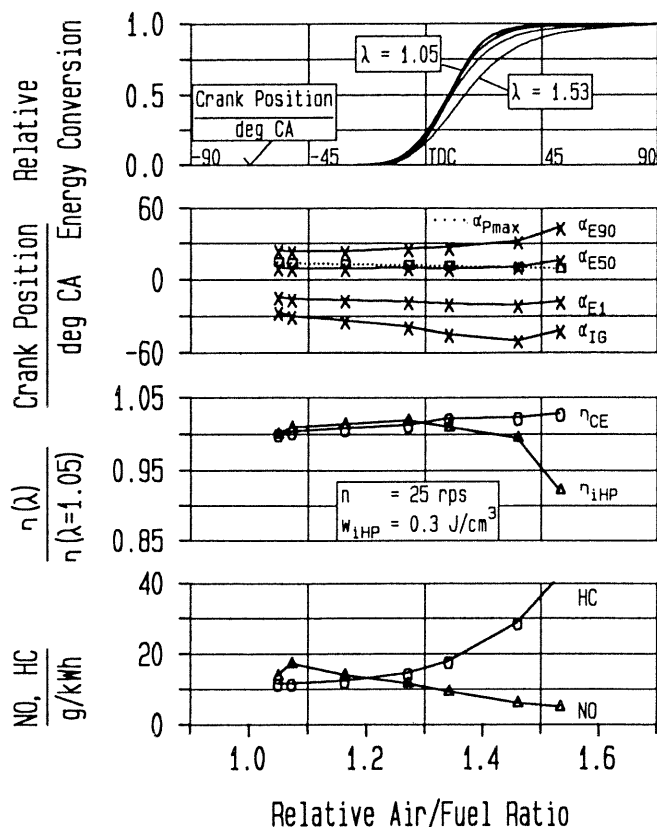


Fig.1 Important values concerning the combustion process

laminar flame speed [5]. When α_{IG} is dictated later by knocking or misfire cycles it is referred to as "restricted" optimum. It causes a delay of the entire combustion process, which is recognizable by the delay of α_{E50} .

Energy conversion

Figure 1 shows the essential relationships regarding the combustion in an SI engine. They are demonstrated at an operating point for the variation of λ , but are also valid for operation with EGR. In the upper diagram, the graphs of the relative energy conversion, calculated from the CP, are shown in relationship to the crank angle. Thereby it is shown that despite the increasing λ , from $\lambda = 1.05$ up to 1.33, the graphs are almost congruent. The reason for that is the "unrestricted" optimum α_{IG} . Deviations become clear only when α_{IG} must be delayed in order to avoid misfire cycles at a maximum λ , here from $\lambda \approx 1.45$ on.

The second diagram of Figure 1 shows the graph of α_{IG} and the individual sections of the energy conversion as they relate to changes in λ . The unrestricted optimum ignition timing of the first five measuring points and the subsequent delay during the further rise of λ can be recognized. As a result, α_{E50} remains constant for the first measuring points and is delayed only at a higher λ .

The position of the maximum cylinder pressure (α_{pmax}) however, is not influenced by the retardation of α_{IG} . This points out the unreliability of this value, which is often used and easy to identify, when operating with high λ .

In the third diagram the indicated high pressure efficiency η_{iHP} as it increases with the rise of λ , and the charge exchange efficiency η_{CE} are shown. The figure,

normalized with the value at a low λ , shows that η_{iHP} increases up to $\lambda \approx 1.3$. From $\lambda \approx 1.45$ η_{iHP} decreases according to the delay of α_{IG} . The rise of η_{CE} indicates the opening of the throttle valve for constant indicated high pressure work (w_{iHP}) with an increasing λ .

In the fourth diagram the rise of λ , up to $\lambda = 1.07$, shows an initial increase of NO, which is then followed by a steady decrease. The increase of HC is slight until $\lambda \approx 1.3$, but becomes greater when λ is raised further.

Thus Figure 1 demonstrates that important relationships concerning the operation of an SI engine can be obtained from the analysis of the CP. The determination of α_{E50} alone allows a statement about the efficiency and the exhaust gas quality, provided that the optimal position of α_{E50} , as well as the relationship between λ and efficiency or emission of NO and HC for the given engine is known.

The new combustion pressure characteristic value

The calculation of α_{E50} from one cycle to the next, however, cannot be done in the computer of an OBM system, and α_{pmax} is not reliable, especially with a high λ and a high rate of EGR [6,7]. Therefore a new model has been developed for the determination of a meaningful characteristic value from the CP.

The calculation of this characteristic value concentrates upon w_{iHP} , which is found by the step-by-step integration of the high pressure loop between compression and expansion for every degree of crank angle, from TDC to BDC, Figure 2. In a subsequent comparison, starting at TDC, the crank position at which 50% of w_{iHP} of the observed cycle is reached is determined. The crank position of this partial integral is referred to as α_{wi50} .

In the second and third diagrams of Figure 2 the behavior of α_{wi50} with increasing λ and rate of EGR is shown, in addition to the crank positions of the partial integrals of 1% and 5%, α_{wi1} and α_{wi5} , respectively, together with α_{E50} . Partial integrals occur later than their corresponding energy conversions because the partial integrals are calculated only from TDC forward. But α_{wi5} and α_{wi50} show very clearly the same dependence upon λ and the rate of EGR as α_{E50} does, although to a lesser degree. This means that in case of an advance or delay of α_{E50} , by 6 °CA, for example, the partial integrals are also advanced or delayed, although by only 2 °CA for α_{wi5} , and by approximately 5 °CA for α_{wi50} . The important fact is, however, that the changes of the partial integrals are always directly correlated with the changes of the energy conversion, and that the given differences remain constant, up to a high λ and high rates of EGR.

The correlation between α_{E50} , and α_{wi5} or α_{wi50} , which is not illustrated here, shows that a constant, very distinct relationship exists - which is independent of engine speed, load, and fuel - between energy conversion and the partial integral of w_{iHP} .

COMBUSTION RADIATION

Due to the fact that suitable pressure transducers are not yet available for mass production use, optical CR is

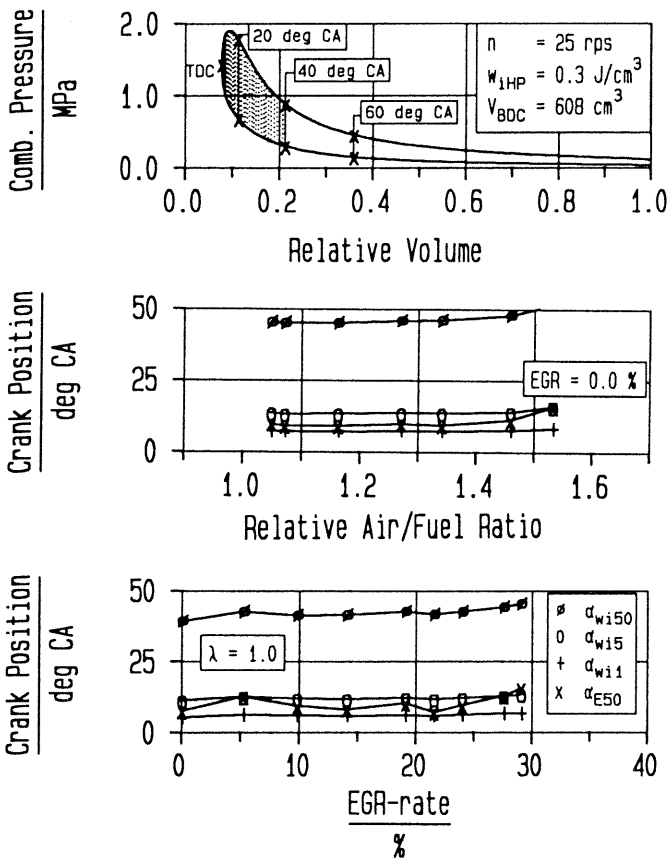


Fig.2 P/V-diagram and comparison of signal behavior

also examined, because its use requires far simpler sensors. This CR is considered both in its entirety, and in its parts, that is, divided spectrally. In addition to providing a statement about the position of the MCP which is nearly as precise as α_{E50} , it also signals the approach to the operation limit when using a "restricted" optimum α_{IG} in order to avoid misfire cycles.

The CR is led from the combustion chamber at a central point and is conveyed to the receiver, an especially sensitive photomultiplier, through a fiber-optic cable. The CR is graphed in relationship to the crank angle.

Polychromatic combustion radiation

In the upper diagram of Figure 3 three graphs of CR demonstrate how with increasing rates of EGR the maximum intensity of the CR decreases, whereas the radiation process begins earlier due to the earlier α_{IG} .

Characteristics calculated from these courses of CR are the crank position of the beginning of the CR (α_{LB}) and the crank position of the maximum of the CR (α_{LM}). The changes of these characteristics with increasing λ or rate of EGR, in comparison to α_{E50} , are shown in the second and third diagrams of Figure 3.

From this it can be seen that α_{LB} reflects the changes of α_{E50} . However with increasing λ , the relationship becomes slight, and is completely missing at a maximum λ . The relationship to α_{E50} is more obvious with increasing rates of EGR, but only above a rate of EGR of approximately 20% does it become very clear. The changes of α_{LM} do not show any relationship to α_{E50} , neither with increasing λ nor with increasing rates of EGR.

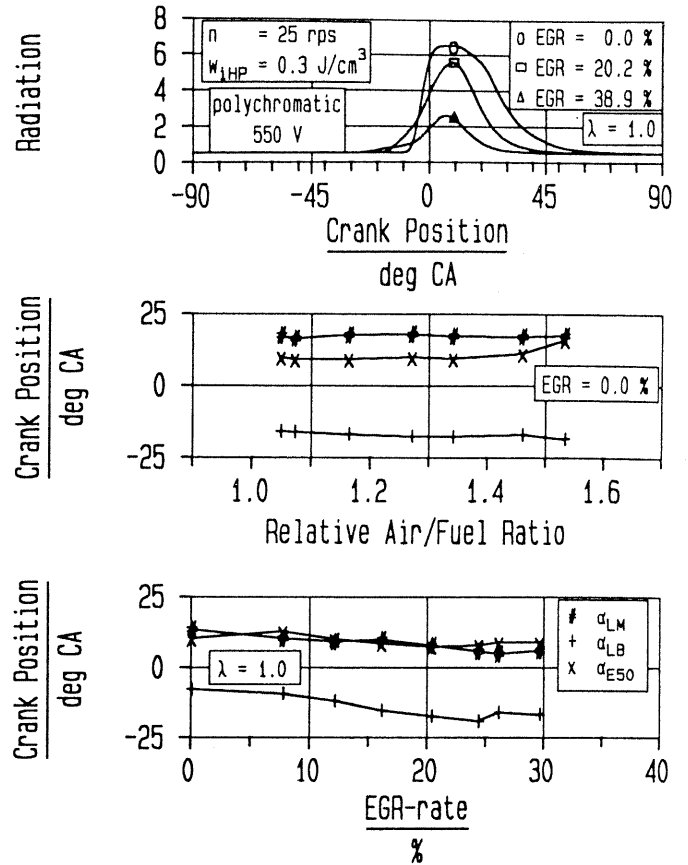


Fig.3 Graphs of CR and comparison of signal behavior

The insufficiency of the statements which were obtained from the CR with regard to the position of the MCP led to an examination of the "relative" CR, see Figure 4. In the upper diagram the graphs show the "relative" CR at different rates of EGR. These graphs result from the integration of the CR over the course of one cycle, and the subsequent normalization. From these normalized graphs, characteristics are calculated. These are the crank positions at which the partial integrals of 5% or 50% of total CR are reached, and are called α_{L5} and α_{L50} .

The behavior of these characteristics with increasing λ or increasing rates of EGR is shown in the second and third diagrams, respectively, of Figure 4, along with α_{E50} . It can be seen that the changes of α_{L5} are directly correlated with those of α_{E50} . Therefore α_{L5} demonstrates a better relationship with α_{E50} than does α_{LB} . The same is true for α_{L50} when compared to α_{LM} . Especially important is that the change to maximum λ or maximum rate of EGR, which for α_{E50} causes a delay - due to the delay of α_{IG} in order to avoid misfire cycles - also leads to a delay of the characteristics of CR.

Monochromatic combustion radiation

In order to obtain further information from the CR, the radiation taken from the combustion chamber was broken down spectrally on the grating of a monochromator. In Figure 5 two spectra of the engine combustion are shown for the previously given point: "unrestricted" optimum α_{IG} in the upper diagram, and a delayed α_{IG} - by approximately 12 °CA - in the lower diagram. Every

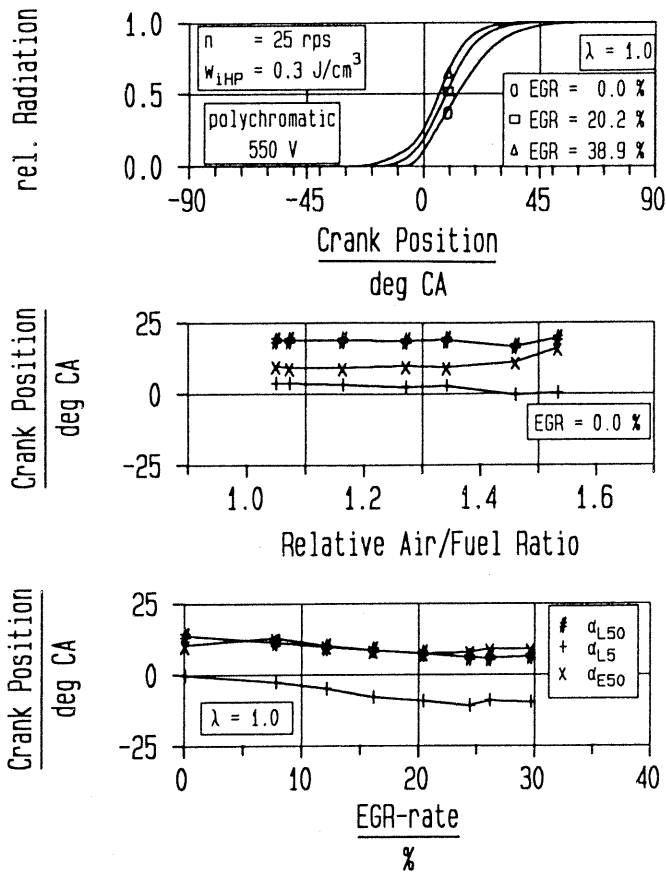


Fig. 4 Graphs of relative CR and comparison of signal behavior

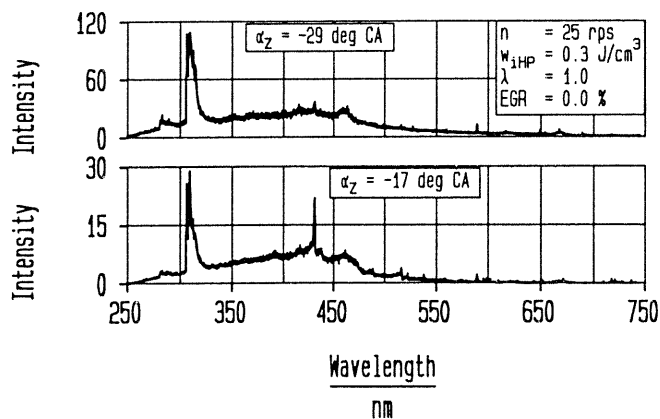


Fig. 5 Spectra of combustion

measuring point is integrated from 25 successive cycles, and the distance between measuring points is 0.1 nm. The points which lie between 300 and 320 nm, as well as those at approximately 430 nm and at approximately 590 nm, are recognizable immediately because of their greater intensity. In addition to these very conspicuous areas in which the spectral lines of the combustion products radiate, there are still more spectral lines, which cannot be seen due to the graph resolution. Because of the recognizability of the single spectral lines in the CR, and because the occurrence of the reaction products during the combustion process might depend upon λ or the rate of EGR, the determination of the characteristics of monochromatic radiation processes provides a further means of examination of combustion with increasing λ or increasing

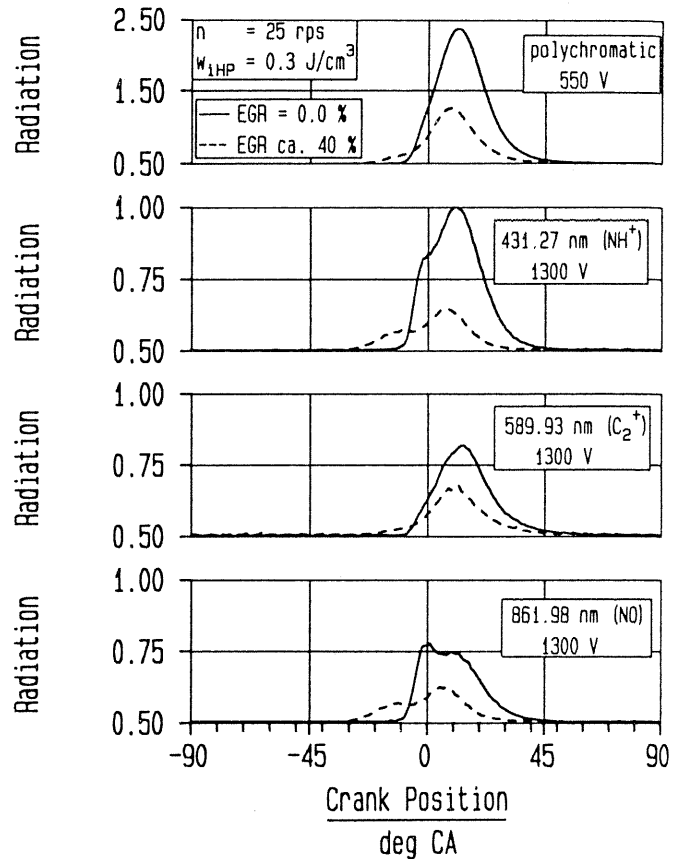


Fig. 6 Graphs of polychromatic and monochromatic CR rates of EGR.

Figure 6 illustrates the development of CR of different wavelengths for the given operating point, once each with and without a maximal rate of EGR, using the photomultiplier voltages shown. An absolute comparison of the various intensities is possible only for the monochromatic CR, because the multiplier which measures polychromatic CR uses a lower voltage. For this reason an ordinate scale is given only for the monochromatic CR in order to allow comparison, but is not assigned an absolute value.

In the upper diagram the uniform polychromatic CR graph is shown without an ordinate scale in order to avoid a comparison with the intensity of the monochromatic CR. The rise of the rate of EGR causes a decrease of the maximum intensity, and to an earlier position of the CR, because of the earlier α_{IG} necessary with a higher rate of EGR.

The change to a wavelength of 431.27 nm, at which NH^+ radiates [8], leads to a differently shaped graph. After a steeper beginning this graph shows a markedly diminished increase of CR, which at a maximum rate of EGR shows the development of a relative maximum. The position of the absolute maximum, however, remains unchanged.

Another monochromatic CR, with a wavelength of 589.93 nm (C_2^+ [8]) does not differ significantly from the graph of polychromatic CR, in terms of its crank position.

In the fourth diagram the graph for a wavelength of 861.98 nm (NO [8]) is shown. This one differs from the polychromatic radiation graph in that it has two maxima.

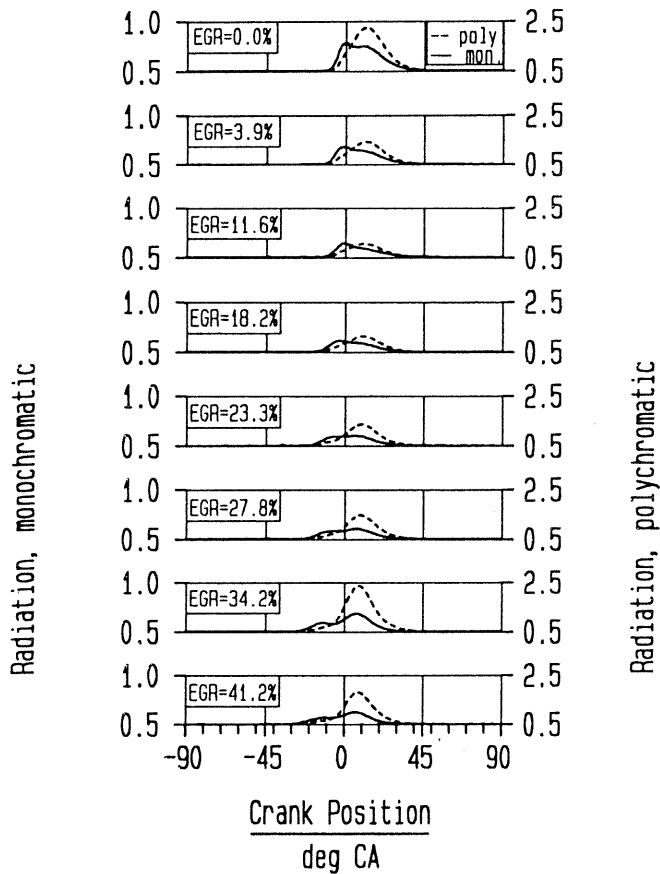


Fig. 7 Graphs of polychromatic and monochromatic (861.98 nm) CR with increasing rate of EGR

Without EGR the first maximum is absolute and the second one is relative. With maximum EGR both maxima shift toward an earlier point, whereby it is significant that now the first maximum is relative and the second one is absolute!

In Figure 7 this change from the first to the second maximum with increasing rates of EGR is especially well demonstrated. Starting at the operating point without EGR, illustrated in the first diagram, an increase up to the maximal rate of EGR within this measurement sequence, shown in the last diagram, takes place. At an EGR rate of 23.3% the existence of both maxima becomes very clearly recognizable. Operation with this rate of EGR marks the limit between operation with "unrestricted" optimum α_{IG} and that with "restricted" optimum α_{IG} , and is at the same time, gives reasonably high efficiency, and low emission of NO, because of the high rate of EGR. The observed change in the position of the absolute radiation maximum at 861.98 nm is found at numerous operating points. It always coincides with the limit of α_{IG} and is made clearly visible by a high standard deviation of α_{LM} .

Figure 8 shows the precise comparison between the characteristics of the polychromatic and the monochromatic CR at 861.98 nm. In the upper diagram the shift of α_{LB} with increasing rates of EGR does not differ greatly between the two kinds of CR. The difference regarding α_{LM} is very clear in the second diagram. With a constant difference of approximately 10 °CA for rates of EGR up to approximately 20%, and with the decreasing

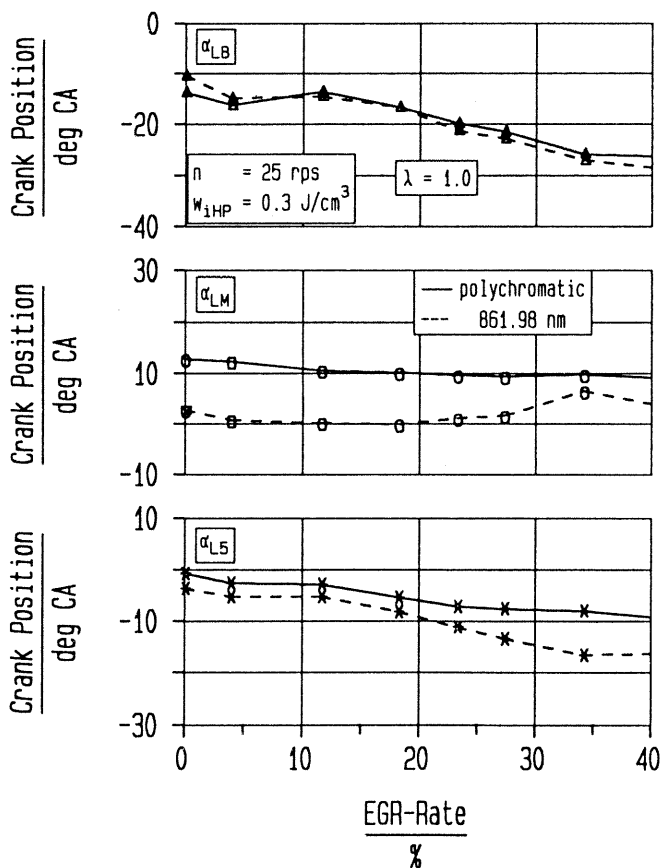


Fig. 8 Behavior of different characteristic values at polychromatic and monochromatic (861.98nm) CR

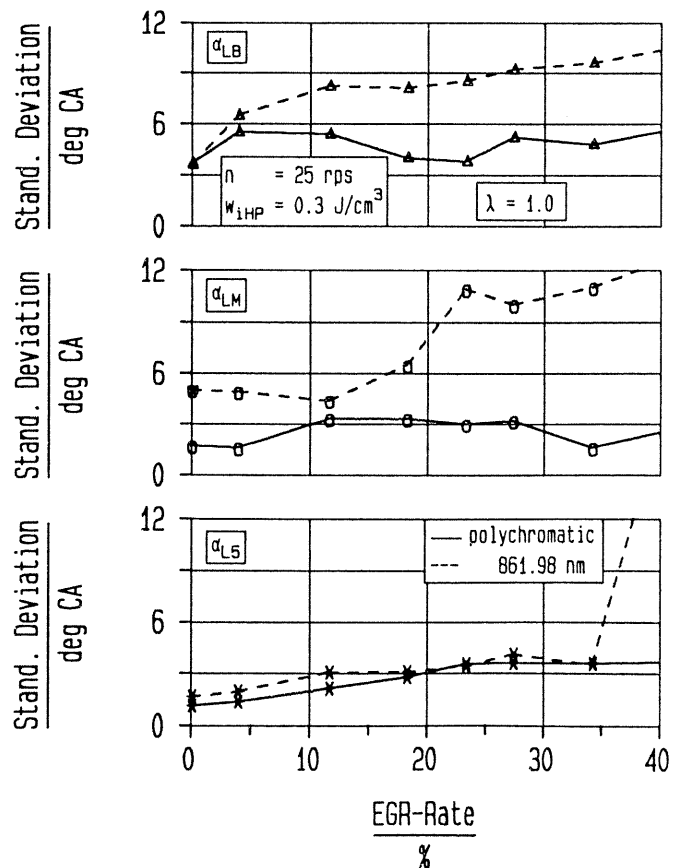


Fig. 9 Standard deviation of different characteristics at polychromatic and monochromatic (861.98nm) CR

difference for the further rise of the rate of EGR, it is possible to quantify the statement inferred from Figure 7. Up to a rate of EGR of approximately 20%, the position of the partial integral of 5% of the monochromatic CR at 861.98 nm changes to a position which is approximately 2°CA earlier. This demonstrates an increase of the monochromatic CR which is only slightly quicker than that of the polychromatic CR. With higher rates of EGR the difference becomes greater, which indicates the quicker increase of monochromatic CR. This relationship can also be explained by the very early relative maximum of monochromatic CR at a high rate of EGR.

DEVIATION OF THE NEW CHARACTERISTICS

The consideration of these values is illustrated in Figure 9. The standard deviation of α_{LB} for the monochromatic CR without EGR is identical to that for the polychromatic CR, but increases uniformly with the rate of EGR, whereas the standard deviation of α_{LB} for the polychromatic CR remains almost unchanged. From that the very strongly restricted area of information of the monochromatic CR is revealed.

The standard deviation of α_{LM} is also nearly independent with regard to the polychromatic CR, whereas for the monochromatic CR the increasing implication of the two maxima is very clearly revealed. The average shape of the graphs in Figure 7 show that for high rates of EGR the second maximum is always the absolute one, whereas

the graph of the standard deviation (in Figure 9) shows that, with regard to its uniform increase above approximately 20% EGR, the first maximum is also often absolute.

Apart from the measuring point at the maximum rate of EGR, the standard deviation of α_{L5} does not clearly distinguish between the values of the polychromatic CR and those of the monochromatic CR. At the last measuring point the standard deviation of α_{L5} amounts to a very high value for the monochromatic CR, thus indicating that the limit for delayed α_{IG} , in order to avoid misfire cycles, is reached.

The relationships are different when the monochromatic CR at 589.93 nm is compared to the polychromatic CR with increasing λ , as is shown in the first two diagrams of Figure 10. Up to $\lambda \approx 1.3$, the standard deviations of the monochromatic values are less than that of the polychromatic CR. With still higher λ , the standard deviation of α_{LB} is somewhat greater, and that of α_{LM} markedly greater, for the monochromatic CR than they are for the polychromatic CR.

For α_{L5} the rise of the standard deviation at maximum relative air/fuel ratios is less pronounced than it is in Figure 9, but still clear enough to recognize the operating limit.

The last two diagrams of Figure 10 illustrate the standard deviations for both kinds of radiation with increasing rates of EGR. For α_{LB} an increase of the standard deviations with increasing rates of EGR can be seen. This increase is generally greater, and even markedly

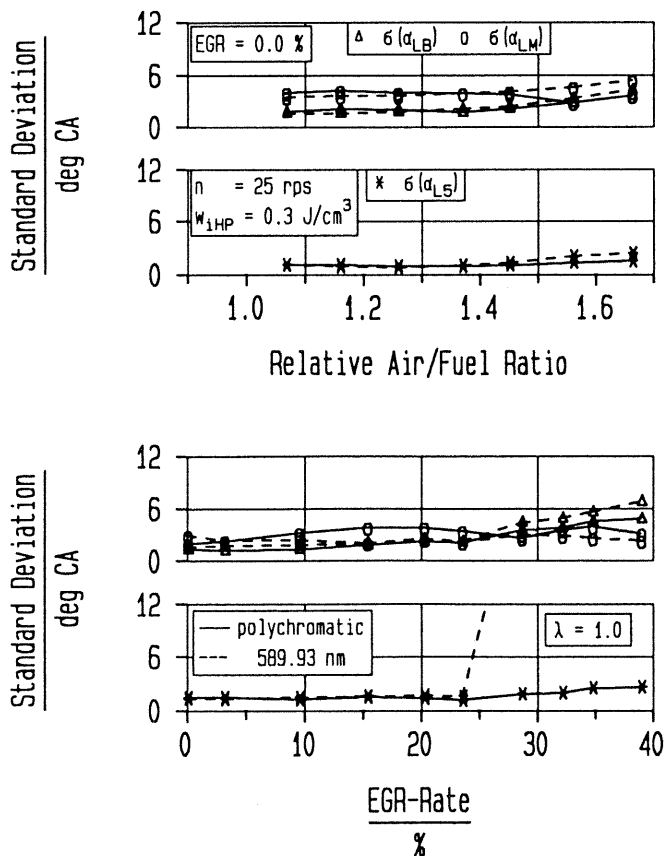


Fig. 10 Standard deviation of different characteristics polychromatic and monochromatic (589.93nm) CR

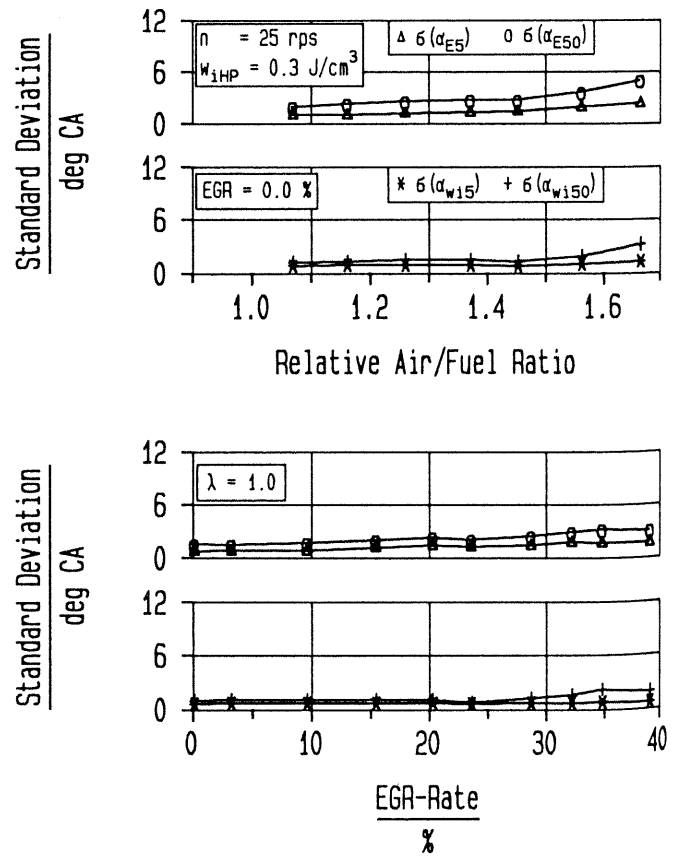


Fig. 11 Standard deviation of characteristic values of the combustion pressure

so above an EGR rate of approximately 24%, for the monochromatic CR at 589.93 nm than it is for the polychromatic CR. For α_{LM} a clear statement cannot be recognized.

Likewise, the standard deviation of α_{L5} for the monochromatic CR increases very strongly compared to the values of the polychromatic CR above an EGR rate of approximately 24%. For this measurement sequence, that is the rate of EGR above which α_{IG} must be delayed in order to avoid misfire cycles.

In Figure 11 the standard deviations of the characteristics of the CP are graphed. Such a clearly recognizable approach to the limit of the "unrestricted" optimal operation as that in Figure 10 cannot be found either for increasing λ , demonstrated in the upper two diagrams, or for increasing rate of EGR, in the lower two diagrams. With increasing λ , an increase of the standard deviations for α_{E50} and α_{wi50} is recognizable, which is caused by the delayed α_{IG} . At maximum rates of EGR, however, the clear delay of α_{IG} leads again to a decreased standard deviation. Therefore it is doubtful that the standard deviations of the characteristics obtained from the CP provide any meaningful statements by which the operating limit might be identified.

SUMMARY

From the CP, and from the CR of individual wavelengths, new characteristics for the control of λ , or of the rate of EGR could be recognized.

From the CP a characteristic value, α_{wi50} , could be obtained by integrating the indicated high pressure loop, section by section. The importance of the crank position of the partial integral of 50% of w_{iHP} was recognized. This value, like α_{E50} , provides reliable information about the position of the MCP. It can be determined much more quickly than α_{E50} and allows reaction from one cycle to the next. It allows the controller to set α_{IG} , the λ and the rate of EGR to produce optimum efficiency and minimum emission of NO and HC. If λ or the rate of EGR is too high for the chosen operating point, it becomes impossible to optimize α_{IG} in order to place the MCP in the required optimum position, a fact which is indicated by α_{wi50} . Therefore, λ or the rate of EGR must be reduced.

With α_{L5} a characteristic value which is independent from the CP was obtained from the polychromatic CR, which again shows a clear relationship to α_{E50} . Examination of monochromatic CR at the wavelengths of 861.98 nm and 589.93 nm confirmed the reliability of this relationship and simultaneously, the standard deviation of α_{L5} provided a signal which indicates the approach to the operating limit at high λ and high rates of EGR.

The good correlation between α_{wi5} , α_{wi50} or the values of the CR and α_{E50} can be seen at every measurement sequence. It is based on the relation between the time changes of mass conversion, represented by α_{E50} , and the resulting work, represented by α_{wi5} and α_{wi50} as well as the values of the CR.

ACKNOWLEDGEMENT

The authors gratefully would like to acknowledge the financial support of the FVV, Frankfurt, Germany.

NOMENCLATURE

Symbol	Descriptions	(Units)
CP	combustion pressure,	(MPa)
CR	combustion radiation	
EGR	exhaust gas recirculation,	(%)
HC	exhaust gas concentration HC,	(g/kWh)
NO	exhaust gas concentration NO,	(g/kWh)
w_{iHP}	indicated high-pressure work,	(J/cm ³)
α_{IG}	ignition timing,	(°CA)
α_{E1}	position of 1 % converted energy,	(°CA)
α_{E5}	position of 5 % converted energy,	(°CA)
α_{E50}	position of 50 % converted energy,	(°CA)
α_{E90}	position of 90 % converted energy,	(°CA)
α_{L5}	position of 5 % CR,	(°CA)
α_{L50}	position of 50 % CR,	(°CA)
α_{LB}	position of the beginning of CR,	(°CA)
α_{LM}	position of the maximum of CR,	(°CA)
α_{pmax}	position of maximum CP,	(°CA)
α_{wi1}	position of 1 % of w_{iHP} ,	(°CA)
α_{wi5}	position of 5 % of w_{iHP} ,	(°CA)
α_{wi50}	position of 50 % of w_{iHP} ,	(°CA)
η_{iHP}	efficiency of w_{iHP} ,	(%)
η_{CE}	efficiency of charge-exchange,	(%)
λ	relative air/fuel ratio,	(1)

REFERENCES

- [1] Bertling H., "Untersuchung der Streuungen im Energieumsetzungsverlauf eines Ottomotors," Thesis TU Braunschweig, 1974
- [2] Müller H., Bertling H., "Programmierte Auswertung von Druckverläufen in Ottomotoren, VDI Fortschrittsberichte 6/30, 1971
- [3] "Low Emission Vehicles/Clean Fuels and New Gasoline Specifications," Progress Report California, Air Resources Board, December 1989
- [4] Malfunction and Diagnostic System Requirements for 1994 and Subsequent Model-Year Passenger Cars, Light-Duty Trucks and Medium-Duty Vehicles with Feedback Fuel Control Systems, Section 1968.1, Title 13, California Code of Regulations
- [5] Kalghatgi G. T., "Spark Ignition, Early Flame Development and Cyclic Variations in I.C. Engines," SAE-paper 870163, 1987
- [6] Martin J. K., Plee S. L., Rembowski D. J. Jr., "Burn Modes and Prior-Cycle Effects on Cyclic Variations in Lean-Burn Spark-Ignition Engine Combustion," SAE 880201, 1988
- [7] Matekunas F. A., "Modes and Measures of Cyclic Combustion Variability," SAE 830337, 1983
- [8] Pearse R. W. B., Gaydon A. G., "The Identification of Molecular Spectra," Chapman & Hall, London, 1976